J. Indian Inst. Sci., July–Aug. 2000, **80**, 319–326.

A new bidirectional topology for electric vehicles

R. GAUTHAM, PRABINDH SUNDARESON AND L. UMANAND
Centre for Electronics Design and Technology, Indian Institute of Science, Bangalore 560 012.
email: lums@cedt.iisc.ernet.in
Phone: 91-80-3600810; Fax: 91-80-3600808

Received on February 2, 2000.

Abstract

This paper describes the development and testing of a novel power converter topology which can be used in systems requiring a high-voltage gain, with features like less stringent requirements on the DC filter capacitor and bidirectional power flow capabilities. This converter is of a modified dual flyback topology and is used as the main converter in an electric two-wheeler (ETW). The advantages, important parameters for the working of the converter and implementation issues are discussed.

Keywords: Flyback converters, ESR, bidirectional conversion.

1. Introduction

Historically, the evolution of power converter topologies has followed that of the development of new power devices.[1–4] These configurations have tried to utilise improved characteristics of power devices to achieve higher power density, higher efficiencies of operation and robustness. One important aspect of these developments is to reduce the filtering requirements by switching at higher frequencies. However, until now, a converter topology that can combine a high-voltage gain with less stringent capacitor requirements has not yet been proven. Research on electric vehicles has broadly taken two paths till now; one along the 'hybrid EV' (HEV),[4] and the other along the 'electrical only' path. A hybrid EV contains a gasoline engine in addition to the electric drive, whereas in 'electrical only' drives, the drive is provided by electricity alone. Various power electronic configurations exist for these drives and induction motor-powered drives have been the focus of research recently. This is mainly because of the higher ruggedness of induction motors. In applications like these, the battery and the inverter need to be interfaced with a high-gain DC–DC converter that provides a high DC link voltage. The size of magnetics can be reduced by switching at high frequencies. However, due to large RMS currents (caused by switching) flowing through the capacitor, the loss due to ESR of the capacitors becomes significant. As a result, the designer needs to add more capacitors and the capacitors become bulky and costly. Further, the DC–DC converter should allow bidirectional power flow to accommodate regenerative braking. This paper addresses these issues.

Section 2 addresses the problems encountered in conventional boost and flyback topologies and discusses the new bidirectional topology, which is well suited for electric vehicle applications.

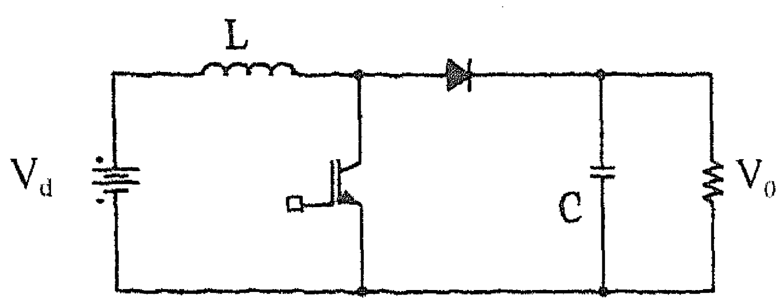

FIG. 1. Boost converter.

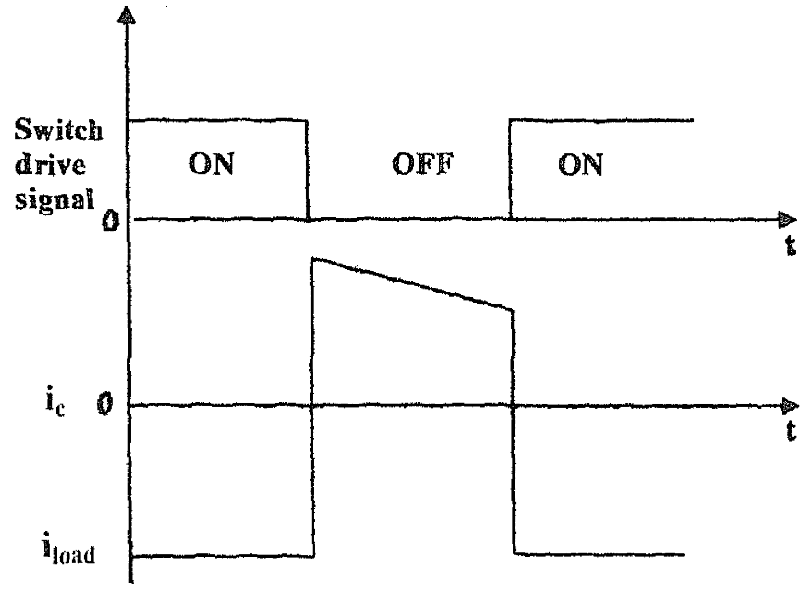

FIG. 2. Boost converter current (I_c).

2. Motivation for the modified dual flyback topology

In the boost configuration, shown in Fig. 1, the energy stored in the inductor is used to charge the capacitor to a voltage higher than the input voltage.

Equation (1) gives the output voltage, where D is the duty cycle of operation:

$$V_0 = \frac{V_d}{(1-D)}. \tag{1}$$

The waveform in Fig. 2 shows the steady-state capacitor current wave shape when the transistor Q is switched on and off.

In our application, the input and output voltages are 48 and 380 V, respectively. The duty cycle from eqn (1) can be calculated to be $D = 0.875$. The RMS current through the capacitor can be calculated from eqn (2):[2]

$$i_{c\,\mathrm{rms}} = \sqrt{\frac{1}{T_s}\left[\int_0^{t_1}(k_1 t + k_2)^2 \mathrm{d}t + \int_{t_1}^{t_2} I_0^2 \mathrm{d}t\right]}, \tag{2}$$

where

$$k_1 = \frac{V_d - V_0}{L}, \qquad k_2 = (I_{in} - I_0) + \frac{\Delta I_L}{2},$$

t_1 = duration of OFF period of the switch and t_2 = total duration of a period of switching. With the above equations, the RMS current through the output capacitor can be calculated at a switching frequency of 20 kHz. The other parameters are:

$P_0 = 2$ kW,

$\Delta I_L = 4.16$ A,

$I_{in} = 41.6$ A,

$I_o = 5.26$ A,

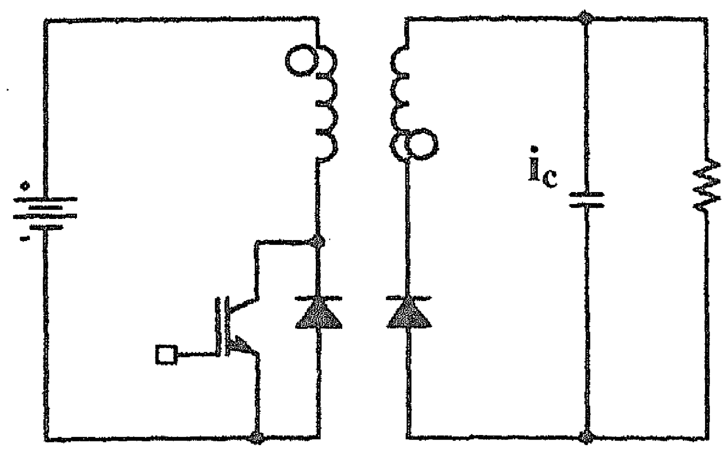

FIG. 3. Nonregenerative flyback converter.

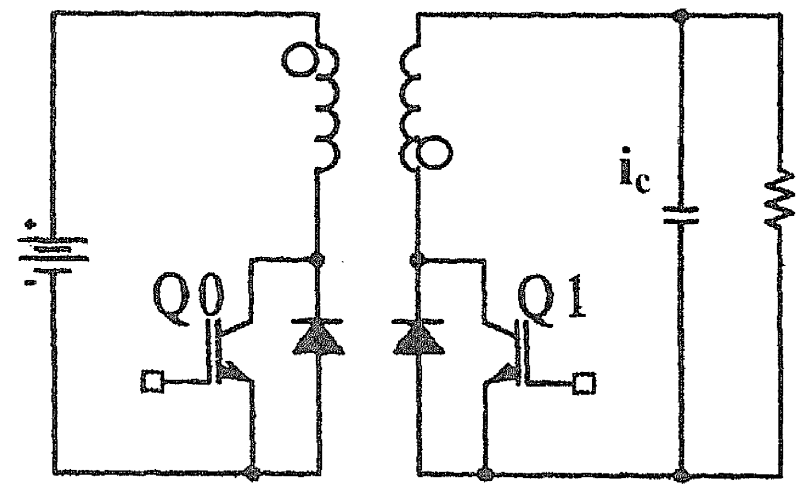

FIG. 4. Regenerative flyback converter.

$t_1 = 6.25\ \mu S$,
$t_2 = 50\ \mu S$.

With these parameters, the RMS current is found to be 13.76 A.

With this configuration, the RMS current through the capacitor is found to be high. This current causes heating in the capacitor due to ESR of the capacitor. As a consequence, the cost and size of the converter becomes prohibitively high. Further, the boost configuration can pump power in only one direction.

In the isolated nonregenerative flyback converter (Fig. 3), the transformer stores the energy when the switch is turned on. This energy is transferred to the output capacitor when the switch is turned off. The wave shape of the capacitor current is similar to that in the boost converter topology (assuming turns ratio of unity). Here, the transformer actually acts as a 'store house' of energy.

In Fig. 4, which is the regenerative flyback configuration, reverse power flow is possible by turning on the switches Q0 and Q1 alternately, depending on the power flow direction. In this configuration, high voltage gain is possible by adjusting the turns ratio of the primary and secondary. Also, bidirectional power flow is possible, and there is isolation between the primary and the secondary.

In a manner similar to that in the boost converter, the high RMS current causes heating in the capacitor due to ESR, and the input current drawn is not pure DC.

3. Principle of the new converter

The new converter is bidirectional. In the forward direction (battery to DC link) of power flow, the converter boosts the DC link voltage. In the reverse direction (DC link to battery) it bucks the DC voltage and charges the battery. Some of the main considerations for choosing the configuration are:

- Reduced RMS current of the DC link capacitor
- Bidirectional power flow
- Galvanic isolation
- Transformer design for fixed 50% duty cycle
- Simplicity of controls for the converter

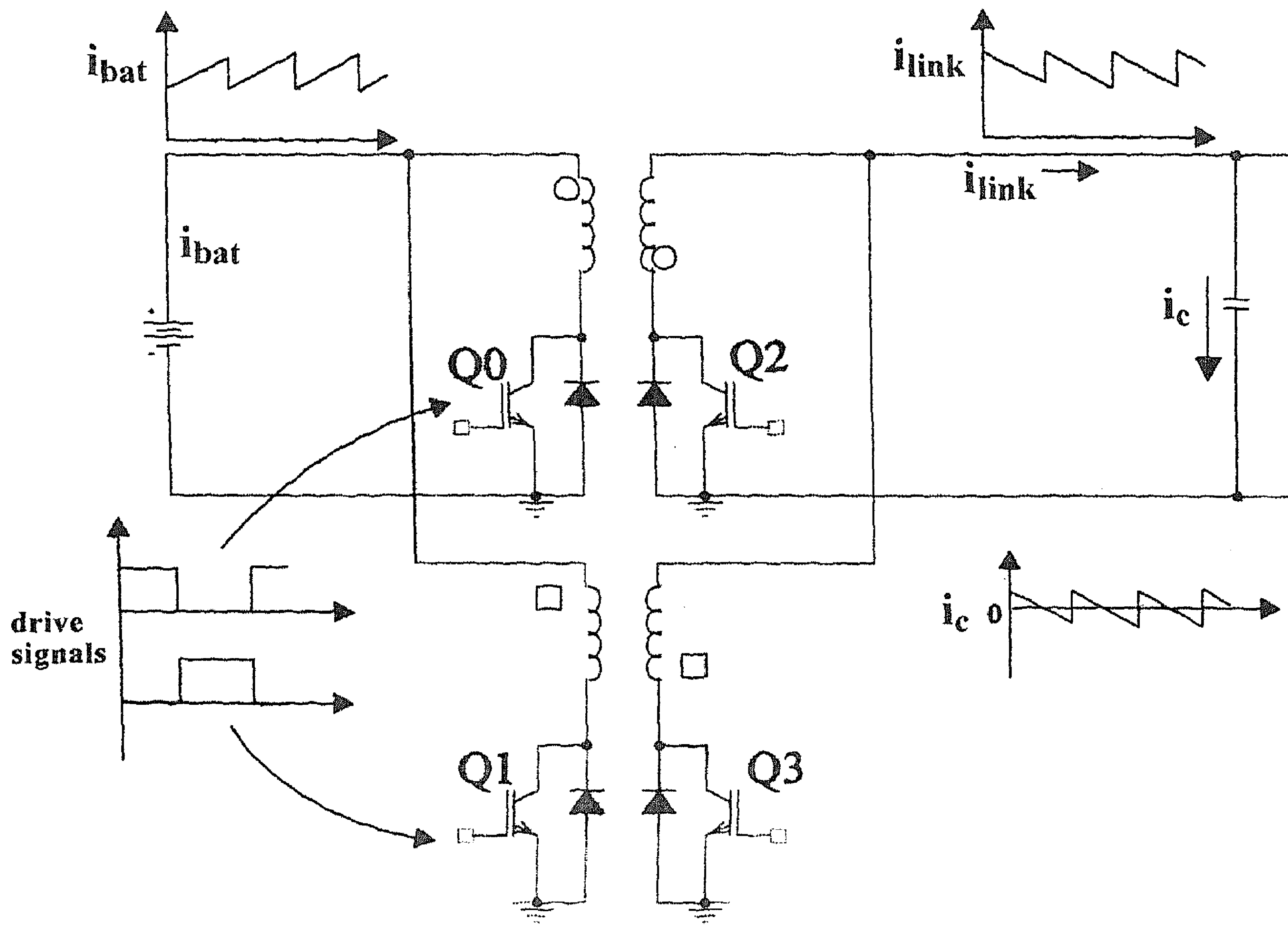

FIG. 5. Principle of the main converter.

If two flyback converters are used in parallel with the switches operated in complementary fashion, then the RMS current in DC link capacitor can be minimised to less than 2 A. The schematic of the main converter is shown in Fig. 5. The ΔI on the primary side is 6.25 A. The ΔI on the secondary side is $6.25/8 = 0.7812$ A, where 8 is the voltage gain between primary and secondary. Now the RMS current through the capacitor is (ref. Appendix 1),

$$\Delta I/\sqrt{12} = 0.7812/\sqrt{12} = 0.225 \text{ A},$$

which is much less than 2% of the capacitor current in the case of boost converter. This will reduce the size and cost of the DC link capacitor. Besides, the size and weight of the magnetics is a minimum. In this configuration the secondary side also needs a switch like IGBT or MOSFET. This will enable power flow in both directions. If power flow in the reverse direction is desired then the switching signal will have to be steered to the secondary side. Driving the IGBTs/MOSFETs of the converter from the control card will not be a problem as no extra isolation is required. The size of the main converter can be further reduced by the usage of high flux density (1.5 T) cores such as METGLAS cores (AlliedSignal). Considering the above advantages, this configuration has been chosen for the main converter.

The switches Q0 and Q1 are operated in complementary fashion with a duty cycle of 50%. When a switch is turned ON, the inductor connected to the respective switch stores the

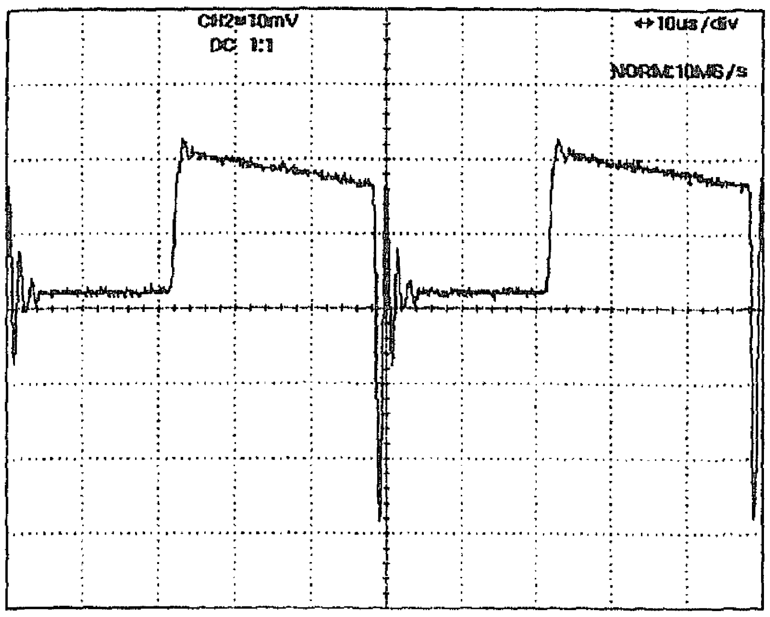

FIG. 6. Current waveform in the secondary winding for single converter (secondary load current of 1 A).

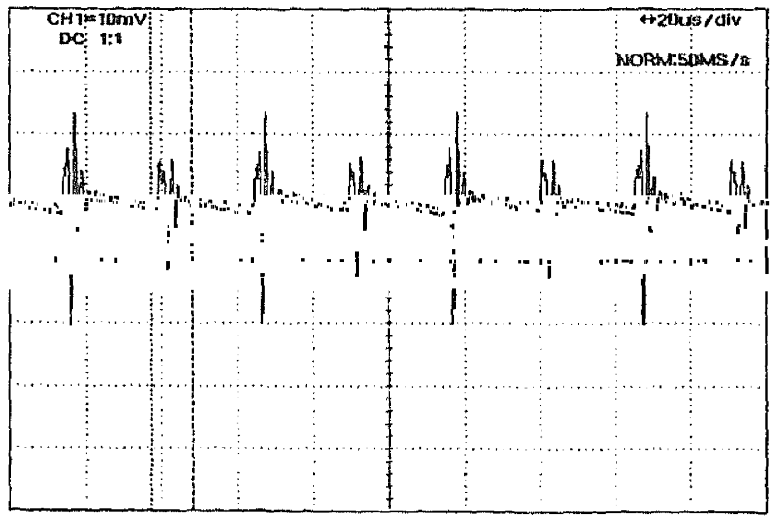

FIG. 7. The sum of the currents in the secondary windings of both the converters. Scale: 1 Amp/Div.

energy. When the switch is turned OFF, the stored energy is passed on to the DC link through the diodes in Q2 and Q3. It can be seen that the capacitor current waveform has very less ripple. When the switches Q0, Q1 are turned off and converter PWM pulses are steered to switches Q2 and Q3, power flow takes place in the reverse direction. In this mode, Q0 and Q1 act as diodes and charge the battery.

For the capacitor current shown in Fig. 4, it can be shown that the RMS current through the capacitor is given by the relation ($\Delta I/\sqrt{12}$) (refer to Appendix 1).

4. Implementation issues

The converter designed as per the above concept was tested in the laboratory. Figure 6 shows the current in the secondary winding for a single converter. It can be seen that the RMS current through the capacitor is large.

This will cause heating in the capacitor due to the ESR of the capacitor. Figure 7 shows the sum of currents in the secondary windings of both the converters. It can be seen that the waveform is a sum of two identical but complementary waveforms of Fig. 6. It can be seen clearly

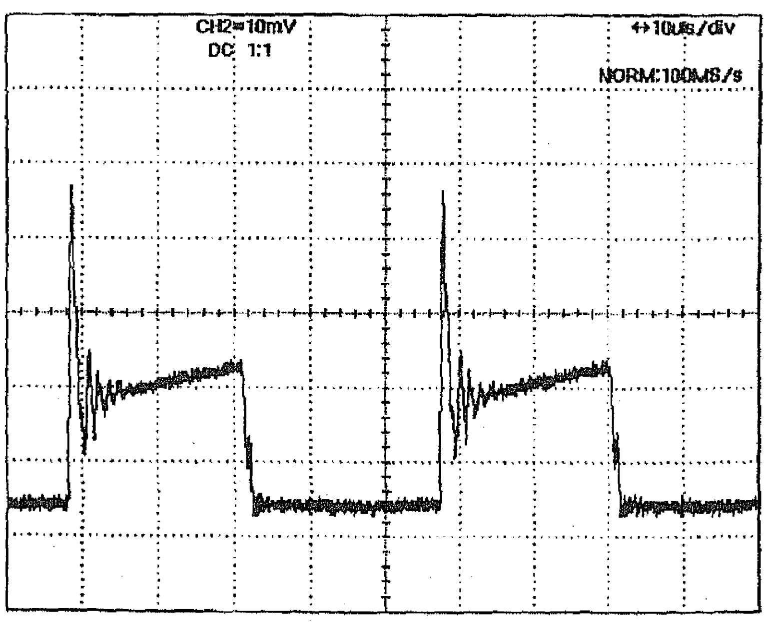

FIG. 8. Primary winding current for a single converter (load current of 1 A). Scale: 5 Amp/Div.

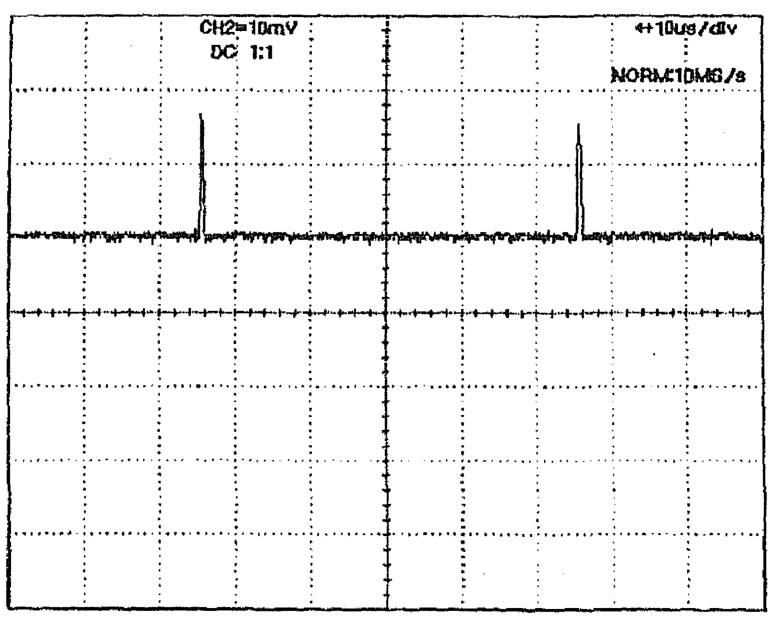

FIG. 9. Current through the primary snubber diode (for a secondary load current is 1 A). Scale: 5 Amp/Div.

that the RMS current of the waveform is very less compared to that in Fig. 6. This current waveform through the DC link capacitor will cause less heating in the capacitors. The spikes and ringing in the current waveform are again due to the reverse recovery time of the diode and the connecting lead inductance. In the ideal case the spikes will be absent.

Figure 8 shows the primary winding current for a single converter. The current was measured using a Hall effect current probe. The current spike during turn-on is due to the slow turn-off of the secondary diode. When the primary MOSFET is on, the current through the winding should be almost linear. Linearity in this region indicates that the core has not saturated. If the core saturates then the current waveform will have a curved shape with a peak at the turn-off. This will cause high currents through the MOSFETs, which may damage the MOSFET.

Figure 9 shows the current through the primary snubber diode. This diode will conduct only during turn-off of the primary MOSFETs. In this case, the peak current at full load is 40 A. Figure 10 shows the input current of a single converter with a 100 μF capacitor connected close to the input terminals of the converter. The capacitor should be of low ESR type. Otherwise the capacitor will heat up due to high RMS currents through it. In the absence of the capacitor at the input terminals there is ringing in the waveforms.

Figure 11 shows the secondary switch waveform. This was recorded using a 1000 : 1 Tektronix probe. The initial spikes, during turn-off, are due to the leakage inductance of the coils. The action of the snubber can be clearly seen during the turn-off as the energy stored in the leakage inductance is dissipated in the snubber in the form of heat. In the absence of the snubber the secondary switch is easily damaged. A similar logic can be applied to the primary side. The primary switch waveform is shown in Fig. 12. The input current with both the converters operating in parallel is shown in Fig. 13. The input current is almost a pure DC but for some small glitches. This is because of the small dead time between the two converters.

5. Conclusion

This paper introduces a new type of bidirectional switching converter topology, which has the feature of reduced ripple current through the output filter capacitor, and has reverse power flow

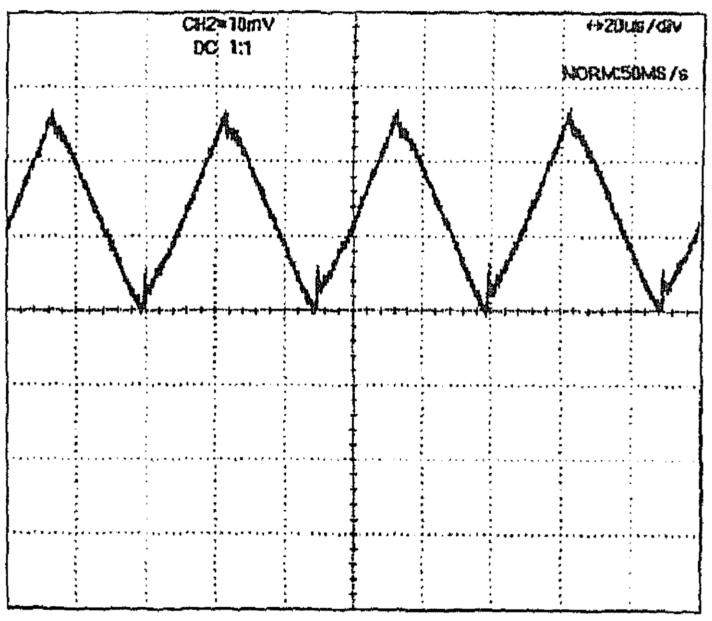

FIG. 10. Input current for a single converter with capacitor across the input lines (for a secondary load of 2 A). Scale: 5Amp/Div.

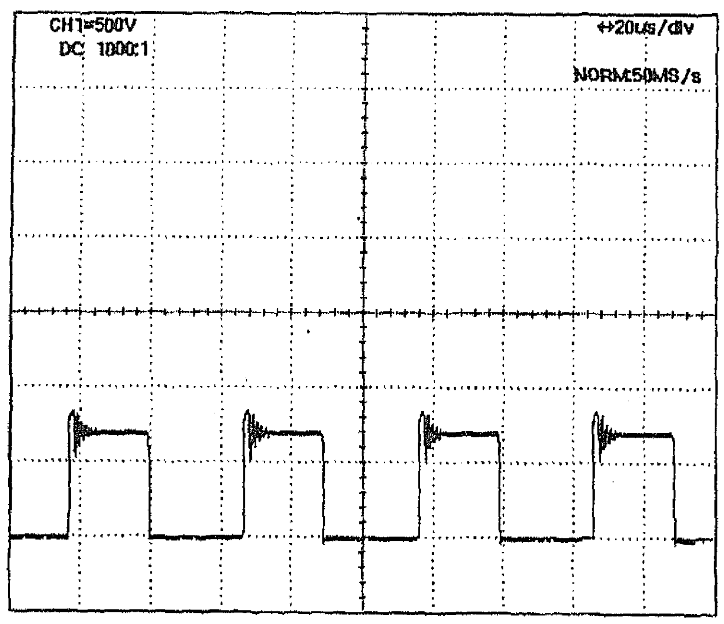

FIG. 11. Secondary MOSFET voltage waveform (at output voltage of 320 V DC).

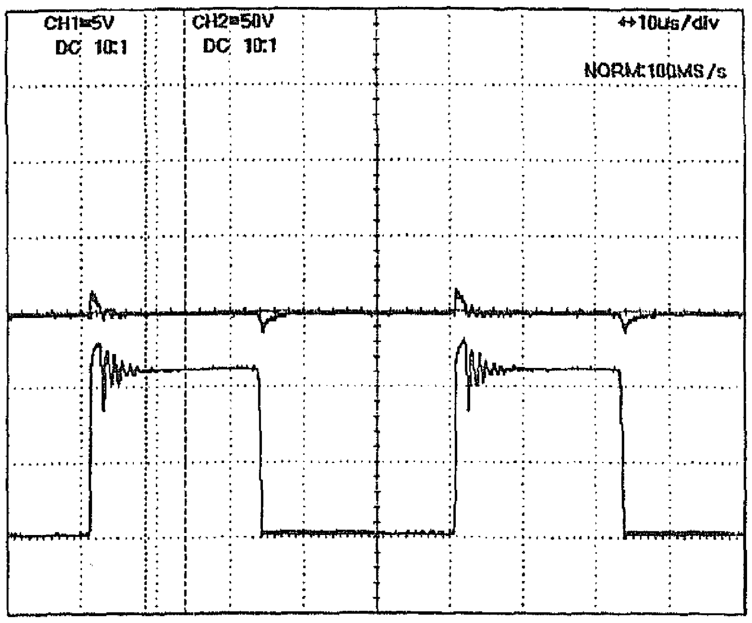

FIG. 12. Primary MOSFET voltage waveform.

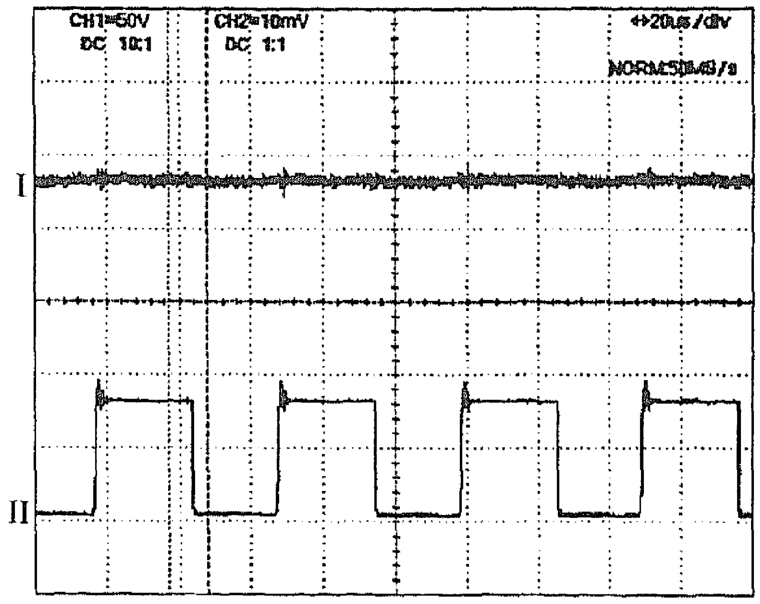

FIG. 13. I. Input current drawn from the battery (both converters in parallel). II. Primary MOSFET voltage of one of the converters.

capabilities, along with high voltage gain. The advantages gained by using this configuration are:

- Reduced RMS current of the DC link capacitor
- Bidirectional power flow
- Galvanic isolation
- Transformer design for fixed 50% duty cycle
- Simplicity of controls for the converter

It has been shown that if two flyback converters are used in parallel with the switches operated in complementary fashion, then the RMS current in DC link capacitor can be minimised to less than 2 A. The results have been recorded and discussed in detail and compared with other topologies.

References

1. CHAN, C. C. AND CHAU, K. T. An overview of power electronics in electric vehicles, *IEEE Trans.*, 1997, **IE-44**, 3–13.
2. NED MOHAN, UNDELAND, T. M. AND ROBBINS, W. P. *Power electronic converters, applications and design*, Wiley, 1995.
3. Electrical Power Research Institutes. www.epri.com.
4. Electric motor bike from EMB, www.electric-motorbike.com.

Appendix 1: Derivation of Equation 3

Referring to Fig. 5, the capacitor current waveform i_c is shown in the figure below. The RMS value of this waveform is derived as follows:

$$I_{\mathrm{Crms}} = \sqrt{\frac{1}{T}\int_0^T i_c^2(t)\,\mathrm{d}t},$$

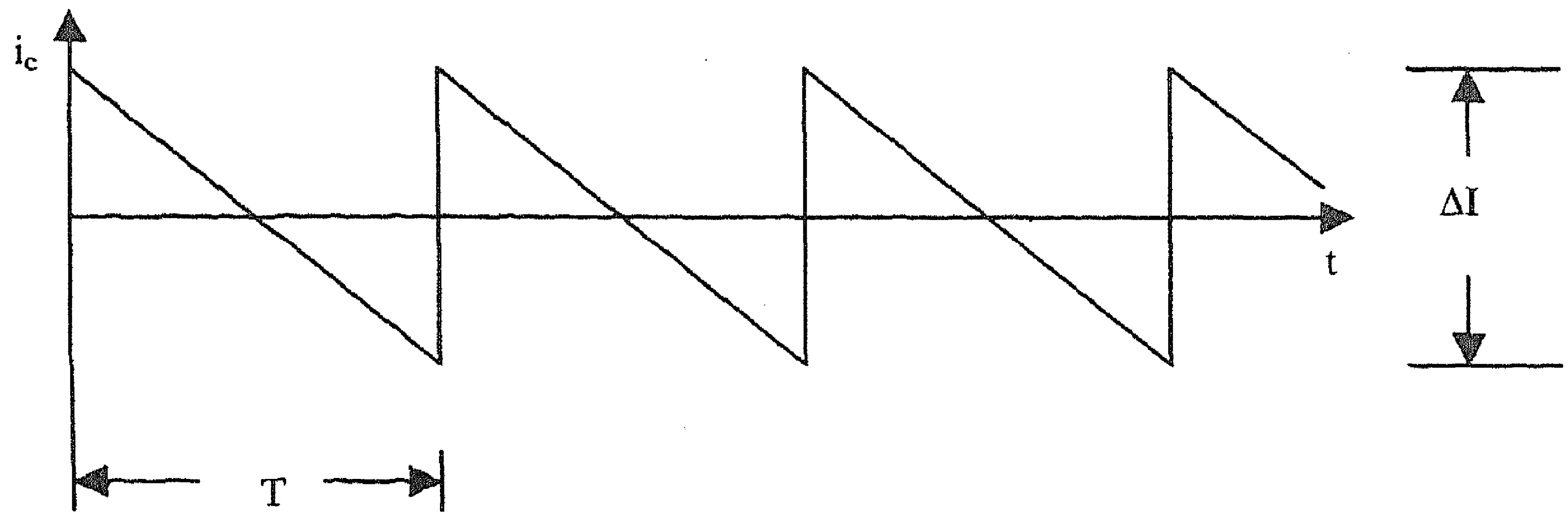

$$I_{\mathrm{Crms}} = \sqrt{(1/T)\left[\int_0^{T/2}\left(\frac{\Delta I}{2}\left(1-\frac{2t}{T}\right)\right)^2 \mathrm{d}t + \int_0^{T/2}\left(\frac{-\Delta I}{2}\right)^2\left(\frac{2t}{T}\right)^2 \mathrm{d}t\right]}$$

$$I_{\mathrm{Crms}} = \sqrt{\frac{\Delta I^2}{4T}\left[\int_0^{T/2}\left(1-\frac{4t}{T}+\frac{4t^2}{T^2}\right)\mathrm{d}t + \int_0^{T/2}\frac{4t^2}{T^2}\,\mathrm{d}t\right]},$$

$$I_{\mathrm{Crms}} = \sqrt{\frac{\Delta I^2}{4T}\left[t-\frac{2t^2}{T}+\frac{4t^3}{3T^2}\right]_0^{T/2} + \left[\frac{4t^3}{3T^2}\right]_0^{T/2}},$$

$$I_{\mathrm{Crms}} = \sqrt{\frac{\Delta I^2}{4T}\left[\frac{T}{6}+\frac{T}{6}\right]},$$

$$I_{\mathrm{Crms}} = \frac{\Delta I}{\sqrt{12}}.$$

Appendix 2: List of symbols

V_d: DC input voltage,
V_0: DC output voltage,
ESR: equivalent series resistance,
T_s: switching period,
D: duty cycle of operation,
T: instantaneous time,
i_{load}: current through load,
ΔI_L: ripple current in inductor current.